Czech Technical University in Prague
Faculty of Nuclear Sciences and Physical Engineering
Department of Physics

RESEARCH PROJECT

K^-–Nucleus Interaction in Relativistic Mean-Field Theory

Daniel Gazda

Supervisor: RNDr. Jiří Mareš, CSc., NPI Řež

Contents

1 Introduction

The subject of the present work is the study of antikaonic properties in nuclear medium. It represents a small part of one of the most important, yet unsolved, problems in hadron physics – how the hadron masses and interactions change within the nuclear medium.

Kaon is a notable example of currently growing interplay among the physics of hadrons, the physics of relativistic heavy-ion collisions, and the physics of compact objects in astrophysics. In all these three mentioned fields kaons play a special role.

The discovery of hadrons with the internal quantum number "strangeness" began a very exciting epoch in particle physics. The major discoveries came unexpectedly or even against expectations of theorists. In 1947, G.D. Rochester and C.C. Butler published two cloud chamber photographs of cosmic ray-induced events. One showing neutral particle decaying into two charged pions, and one decaying into a charged pion and something neutral. More examples of these "V-particles" were slowly coming. The first breakthrough was obtained at Caltech, where a cloud chamber was taken up Mount Wilson, for greater cosmic ray exposure. In 1950, 30 charged and 4 neutral V-particles were reported. Inspired by this, numerous mountaintop observations were made over the next several years. The decays were extremely slow of the order 10^{-10} seconds. However, production in pion–proton reactions proceeds much faster, with a time scale of 10^{-23} seconds. The problem of this mismatch was solved by A. Pais who postulated the new quantum number called "strangeness" which is conserved in strong interactions but violated by the weak interactions. Strange particles appear copiously due to "associated production" of a strange and antistrange particle together. Two different decays were found for charged strange mesons: $\theta^+ \to \pi^+\pi^0$ and $\tau^+ \to \pi^+\pi^+\pi^-$. Since the two final states have different parity it was thought that initial sates should also have different parities, and hence be two distinct particles. However, with increasingly precise measurements, there were found to be no difference between their masses and lifetimes, indicating that they are the same particle. This was known as the $\theta-\tau$ puzzle. It was resolved only by the discovery of parity violation in weak interactions. Since the mesons decay through weak interactions, parity need not to be conserved, and the two decays may be caused by the same particle, now called the K^+.

Initially it was thought that although parity was violated, CP symmetry was conserved. The CP violation was first observed in the context of neutral kaon mixing, although this phenomenon does not require CP violation. The CP violation due to mixing of K^0 and its antiparticle is known as indirect CP violation. There is also a direct CP violation effect, in which the CP violation occurs during the decay itself. Moreover, the CP violation found in the K^0 system is closely related to the violation of the T invariance via CPT theorem. For details see e.g. Ref. [1].

Ever since the pioneering work of Kaplan and Nelson [2, 3] on the possibility of kaon condensation in nuclear matter, a huge amount of theoretical effort has been devoted to the study of kaon properties in dense matter. At present, the main evidence for a strong

in-medium modification of the K^-N interaction is due to to the enhanced production of K^- mesons observed in subthreshold and near-threshold heavy-ion collisions in the KaoS experiment at GSI [4-6]. Using several methods, such as chiral perturbation theory (χPT) [7-9], RMF model [8-11], chiral coupled channel model [12, 13], chiral unitary model [14, 15] or other chiral model [16, 17], and the phenomenological model by fitting the K^-–atomic data using a density dependent optical potential (DD) [18-20] etc., a strong attractive K^-–nucleus potential at threshold is predicted. These calculations show strong dependence on the applied model. The DD model gives the deepest K^-–nucleus potential in the range of $\sim 150 - 200$ MeV [18-20]. The chiral coupled channel model predicts the potential in the range of $\sim 85 - 120$ MeV [9, 11, 14], close to that by RMF model. The chiral models give shallower K^-–nucleus potential in the range of $\sim 50 - 70$ MeV [9, 14-17].

The issue of possible existence of K^-–nuclear deeply bound states has attracted considerable attention recently [21]. Several experimental reports claimed evidence for peaks that are assigned to relatively narrow ($\Gamma_{K^-} < 25$ MeV) and deep ($B_{K^-} \gtrsim 100$ MeV) K^-–nuclear states [22-24]. Recent FINUDA experiment [25] suggested deep binding of K^- in Li and C. An alternative, more conventional interpretation of the FINUDA events in terms of Fermi motion of the initial pp pair and the nuclear final-state interaction of the emitted Λp pair was presented in Ref. [26]. These reports again highlighted the question of how attractive the K^-–nucleus interaction is below the K^-N threshold. Obviously, the "shallow"–type potentials cannot generate deeply bound nuclear states in the energy range $B_{K^-} \sim 100 - 200$ MeV, whereas the deep potentials might do. The distinction between 'deep' and 'shallow' K^-–nucleus potential become somewhat fuzzy within a dynamical approach, used in this work, which allows for polarization of the nucleus by the strong K^-–nucleus interaction. The depth of the K^-–nucleus potential becomes then state dependent, thus depending on the binding energy B_{K^-}.

In recent years, many investigations have been devoted to a relativistic description of the ground state properties of nuclei. In analogy to a very early idea of Teller et al. [27-29] Walecka and his collaborators [30, 31] developed a relativistic quantum field theory for a nuclear many-body problem. Taking as their starting point a Lagrangian density containing nucleonic and mesonic degrees of freedom, they avoid the complicated procedure of deriving first a bare nucleon-nucleon interaction, which reproduces nucleon-nucleon scattering data, and then using this force in a Bruckener-Hartee-Fock calculations. Instead, they, assuming mean-field approximation, fitted the coupling constants and unknown meson masses to reproduce the data of nuclear matter and a few finite nuclei. The relativistic mean-field (RMF) model is therefore a phenomenological effective theory for a quantitative description of nuclear properties. It is considered to be relativistic generalization of its non-relativistic counterparts, such as the Skyrme force [32] or the Gogny force [33], which have been extremely successful in describing nuclear structure and low-energy dynamics within the Hartee-Fock or time-dependent Hartee-Fock approach [34]. In contrary the RMF uses (effective) mesonic degrees of freedom rather than concept of instantaneous force. It was shown that RMF model is as flexible and powerful as the non-relativistic models with the additional bonus that some relativistic effects, such as the spin-orbit force, come out more

naturally. This method has turned out to be very successful tool for the description of many nuclear properties. Binding energies and nuclear charge radii are reproduced to within a few percent and the density distributions of doubly magic spherical nuclei are in excellent agreement with electron scattering data. Besides the ground state properties of spherical nuclei, the single particle spectra have been investigated and the right ordering of levels obtained. The bulk of the RMF applications have been devoted to nuclear matter and few spherical doubly magic nuclei but in recent years the applications have been successfully extended to deformed nuclei, unstable nuclei, hypernuclei and other bound systems.

The next section contains the K^-–nucleus RMF methodology used in this work and discussion of its extension to describe absorptive interactions by which the K^-–nuclear states acquire a width. In section 3 we show and discuss the results of calculations and the summary is given in section 4.

2 Methodology

The theoretical framework adopted in this work is a relativistic mean field (RMF) model for a system of nucleons and one K^- meson interacting through the exchange of scalar and vector meson fields. The calculation is made self-consistent by successively allowing the K^- to polarize the nucleus and the polarized nucleus to enhance the K^-–nuclear interaction.

K^-–absorption modes are included within a $t\rho$ optical model approach where the density plays a dynamical role, and the constant t which is constrained near threshold by K^-–atom data follows the kinematical phase-space reduction for a deeply bound K^-–states.

2.1 The RMF Model

Our starting point is a model of relativistic quantum field theory, proposed by Walecka and collaborators [31], which we have extended to incorporate (anti)kaonic sector, and which describes nucleons as Dirac fields (ψ_i) and kaon as Klein-Gordon field (K) interacting trough the exchange of meson fields: Isoscalar-scalar meson (σ) is responsible for the medium range attraction between nucleons, isoscalar-vector mesons (ω) mediates the short-range repulsion, isovector-vector mesons (ρ) allows to adjust isovector properties, and the photon, of course, accounts for the known electro-magnetic interaction. An isovector-scalar δ-meson is left out since it does not improve the model. The π- and η-mesons with unnatural parity are not included because we are working with nuclear states which have well-defined parity [35]. We therefore start from the Lagrangian density

$$\begin{aligned}
\mathcal{L} = & \bar{\psi}_i(\,\mathrm{i}\,\partial\!\!\!/ - m_N)\,\psi_i \\
& + \frac{1}{2}\partial_\mu\,\sigma\partial^\mu\sigma - \frac{1}{2}m_\sigma^2\sigma^2 - g_{\sigma N}\,\bar{\psi}_i\psi_i\sigma - \frac{1}{3}g_2\sigma^3 - \frac{1}{4}g_3\sigma^4 \\
& - \frac{1}{4}\Omega_{\mu\nu}\Omega^{\mu\nu} + \frac{1}{2}m_\omega^2\omega_\mu\omega^\mu - g_{\omega N}\,\bar{\psi}_i\gamma_\mu\psi_i\omega^\mu + \frac{1}{4}\,d\,(\omega_\mu\omega^\mu)^2 \\
& - \frac{1}{4}\vec{R}_{\mu\nu}\cdot\vec{R}^{\mu\nu} + \frac{1}{2}m_\rho^2\,\vec{\rho}_\mu\cdot\vec{\rho}^{\,\mu} - g_{\rho N}\,\bar{\psi}_i\gamma_\mu\vec{\tau}\psi_i\cdot\vec{\rho}^{\,\mu} \\
& - \frac{1}{4}F_{\mu\nu}F^{\mu\nu} - e\,\bar{\psi}_i\gamma_\mu\,\tfrac{1}{2}(1+\tau_3)\psi_i A^\mu \\
& + (\mathcal{D}_\mu K)^\dagger(\mathcal{D}^\mu K) - m_K^2 K^\dagger K - g_{\sigma K}\,m_K K^\dagger K\sigma\,, \qquad (2.1)
\end{aligned}$$

where we use the standard summation convention and the sum runs over all nucleons. Isovector quantities are indicated by arrows, the dot denotes inner product, and $\vec{\tau}$ indicates the usual triplet of the Pauli matrices[1]. Moreover m_N, m_σ, m_ω, m_ρ and m_K are the nucleon, the σ-, the ω-, the ρ- and the K-meson masses respectively. $g_{\sigma N}$, $g_{\omega N}$, $g_{\rho N}$, e, $g_{\sigma K}$ are the coupling constants for the σ-, the ω-, the ρ-meson and the photon with respect to the nucleon, respectively, $g_{\sigma K}$ is the σ-meson-kaon coupling constant.

[1] See appendix A.

The field tensors for the vector mesons and the photon field are given by

$$\begin{aligned}
\Omega_{\mu\nu} &\equiv \partial_\mu \omega_\nu - \partial_\nu \omega_\mu \\
\vec{R}_{\mu\nu} &\equiv \partial_\mu \vec{\rho}_\nu - \partial_\nu \vec{\rho}_\mu - g_{\rho N}\, \vec{\rho}_\mu \times \vec{\rho}_\nu \\
F_{\mu\nu} &\equiv \partial_\mu A_\nu - \partial_\nu A_\mu
\end{aligned} \tag{2.2}$$

and the covariant derivative $\mathcal{D}_\mu$ is defined as

$$\mathcal{D}_\mu \equiv \partial_\mu + \mathrm{i}\, g_{\omega K}\, \omega_\mu + \mathrm{i}\, g_{\rho K}\, \vec{\tau} \cdot \vec{\rho}_\mu + \mathrm{i}\, e\, \tfrac{1}{2}(1+\tau_3) A_\mu \,, \tag{2.3}$$

where $g_{\omega K}$, $g_{\rho K}$ and e are the ω-, the ρ-meson and the photon coupling constants with respect to the kaon.

The classical Hamiltonian variational principle[2]

$$\delta \int \mathrm{d}^4x\, \mathcal{L}\left[q_j(x), \partial_\mu q_j(x)\right] = 0 \Leftrightarrow \frac{\partial}{\partial x^\mu}\left[\frac{\delta \mathcal{L}}{\delta \frac{\partial q_j}{\partial x^\mu}}\right] - \frac{\delta \mathcal{L}}{\delta q_j} = 0 \,, \tag{2.4}$$

where q_j is one of the generalized coordinates (ψ_i, $\psi_i^\dagger$, K, $K^\dagger$, σ, ω_μ, $\vec{\rho}_\mu$, A_μ), gives the equations of motion for these fields :

The Dirac equations for nucleons

$$[\,\mathrm{i}\,\partial\!\!\!/ - m_N - g_{\sigma N}\,\sigma - g_{\omega N}\,\gamma_\mu \omega^\mu - g_{\rho N}\,\gamma_\mu \vec{\tau} \cdot \vec{\rho}^{\,\mu} - e\,\gamma_\mu \tfrac{1}{2}(1+\tau_3)]\psi_i = 0 \,, \tag{2.5}$$

and the Klein-Gordon equations for the kaon

$$(\mathcal{D}_\mu^\dagger \mathcal{D}^\mu) K = -g_{\sigma K}\, m_K \sigma K \tag{2.6}$$

and for the meson fields

$$(\partial_\nu \partial^\nu + m_\sigma^2)\sigma = -\, g_{\sigma N}\, \bar{\psi}_i \psi_i - g_2 \sigma^2 - g_3 \sigma^3 - g_{\sigma K}\, m_K K^\dagger K \tag{2.7}$$

$$\begin{aligned}
(\partial_\nu \partial^\nu + m_\omega^2)\omega_\mu =\, & g_{\omega N}\, \bar{\psi}_i \gamma_\mu \psi_i - d\, \omega_\mu (\omega_\nu \omega^\nu) + \mathrm{i}\, g_{\omega K}\, (K^\dagger \overleftrightarrow{\partial_\mu} K) - 2 g_{\omega K}{}^2 \omega_\mu K^\dagger K \\
& - 2 g_{\omega K}\, g_{\rho K}\, (K^\dagger \vec{\tau} K) \cdot \vec{\rho}_\mu - 2e\, g_{\omega K}\, [K^\dagger \tfrac{1}{2}(1+\tau_3) K] A_\mu
\end{aligned} \tag{2.8}$$

$$\begin{aligned}
(\partial_\nu \partial^\nu + m_\rho^2)\vec{\rho}_\mu =\, & g_{\rho N}\, \bar{\psi}_i \gamma_\mu \vec{\tau} \psi_i + \mathrm{i}\, g_{\rho K}\, (K^\dagger \vec{\tau} \overleftrightarrow{\partial_\mu} K) - 2 g_{\rho K}{}^2 K^\dagger K \vec{\rho}_\mu \\
& - 2e\, g_{\rho K}\, A_\mu [K^\dagger \vec{\tau} \tfrac{1}{2}(1+\tau_3) K] + 2 g_{\omega K}\, g_{\rho K}\, \omega_\mu (K^\dagger K)
\end{aligned} \tag{2.9}$$

$$\begin{aligned}
\partial_\nu \partial^\nu A_\mu =\, & e\, \bar{\psi}_i \gamma_\mu\, \tfrac{1}{2}(1+\tau_3) \psi_i + \mathrm{i}\, e\, [K^\dagger \overleftrightarrow{\partial_\mu} \tfrac{1}{2}(1+\tau_3) K] \\
& - e^{\,2} A_\mu [K^\dagger \tfrac{1}{2}(1+\tau_3) K] - 2e\, g_{\omega K}\, \omega_\mu [K^\dagger \tfrac{1}{2}(1+\tau_3) K] \\
& - 2e\, g_{\rho K}\, \vec{\rho}_\mu \cdot [K^\dagger \vec{\tau} \tfrac{1}{2}(1+\tau_3) K] \,.
\end{aligned} \tag{2.10}$$

[2]See e.g. Ref. [36].

Equations (2.5)-(2.10) are nonlinear quantum fields equations, and their exact solutions are very complicated. Moreover, since we expect the coupling constants (except e) to be large, perturbative approaches are not useful. Fortunately, there is an approximative solution that should become increasingly valid, as the nuclear density increases [31]. When the source terms on the right-hand-sides of equations (2.7)-(2.10) are large, the meson field operators can be replaced by their expectation values, which are classical fields.

Further, symmetries simplify the calculations considerably. We are looking for the nuclear ground states[3] of doubly magic nuclei, which are spherically symmetric. The presence of the antikaon breaks the spherical symmetry negligibly because it is assumed to be in the s–state. Rotational invariance implies that the expectation value of space-like components of vector fields and densities vanish. In this case meson fields and densities also depend only on the radial coordinate r. The electromagnetic charge conservation prohibits charged components of the ρ-meson field from appearing as classical fields. The mean-field equations are further greatly simplified due to stationarity – all time derivatives of meson fields vanish, i.e. :

$$\begin{aligned}
\sigma(x) &\to \sigma_0(r) \\
\omega_\mu(x) &\to \delta_{\mu 0}\,\omega_0(r) \\
\rho^i_\mu(x) &\to \delta_{\mu 0}\,\delta^{i3}\rho_0(r) \\
A_\mu(x) &\to \delta_{\mu 0}\,A_0(r)\;.
\end{aligned} \tag{2.11}$$

With these assumptions we can rewrite the Lagrangian density (2.1)

$$\begin{aligned}
\mathcal{L}^{(MFT)} = &\bar\psi_i(\mathrm{i}\,\partial\!\!\!/ - m_N - g_{\sigma N}\,\sigma_0 - g_{\omega N}\,\gamma_0\,\omega_0 - g_{\rho N}\,\gamma_0\tau_3\rho_0 - e\,\gamma_0\frac{1-\tau_3}{2}A_0)\psi_i \\
&- \frac{1}{3}g_2\,\sigma_0^3 - \frac{1}{4}g_3\,\sigma_0^4 + \frac{1}{4}d\,\omega_0^4 \\
&- \frac{1}{2}[(\nabla_i\sigma_0)^2 + m_\sigma^2\sigma^2] + \frac{1}{2}[(\nabla_i\omega_0)^2 + m_\omega^2\omega^2] + \frac{1}{2}[(\nabla_i\rho_0)^2 + m_\rho^2\rho^2] \\
&- [(\nabla_i K^*)(\nabla_i K) + m_K^2 K^* K] - g_{\sigma K}\,m_K\sigma K^* K \\
&+ (E_{K^-} + g_{\omega K}\,\omega_0 + g_{\rho K}\,\rho_0 + e\,A_0)^2 K^* K
\end{aligned} \tag{2.12}$$

and consequently equations of motion

$$[-\mathrm{i}\,\alpha_j\nabla_j + (m_N + g_{\sigma N}\,\sigma)\beta + g_{\omega N}\,\omega_0 + g_{\rho N}\,\tau_3\rho_0 + e\,\frac{1-\tau_3}{2}A_0]\psi_i = \varepsilon_i\psi_i \tag{2.13}$$

$$\begin{aligned}
(-\triangle + m_\sigma^2)\sigma_0 = &- g_{\sigma N}\;{<\!:}\,\bar\psi_i\psi_i\,{:\!>} - g_2\,\sigma^2 - g_3\,\sigma^3 \\
&- g_{\sigma K}\,m_K K^* K
\end{aligned} \tag{2.14}$$

$$\begin{aligned}
(-\triangle + m_\omega^2)\omega_0 = &\, g_{\omega N}\;{<\!:}\,\psi_i^\dagger\psi_i\,{:\!>} - d\,\omega_0^3 \\
&- 2g_{\omega K}\,(E_{K^-} + g_{\omega K}\,\omega_0 + g_{\rho K}\,\rho_0 + e\,A_0)K^* K
\end{aligned} \tag{2.15}$$

$$\begin{aligned}
(-\triangle + m_\rho^2)\rho_0 = &\, g_{\rho N}\;{<\!:}\,\psi_i^\dagger\tau_3\psi_i\,{:\!>} \\
&- 2g_{\rho K}\,(E_{K^-} + g_{\omega K}\,\omega_0 + g_{\rho K}\,\rho_0 + e\,A_0)K^* K
\end{aligned} \tag{2.16}$$

[3] or more general, stationary states

$$-\triangle A_0 = e \; <: \psi_i^\dagger \frac{1-\tau_3}{2} \psi_i :> \\ - 2e\,(E_{K^-} + g_{\omega K}\,\omega_0 + g_{\rho K}\,\rho_0 + e\,A_0) K^* K \tag{2.17}$$

$$(-\triangle + m_K^2) K^* = [-g_{\sigma K}\, m_K \sigma + (E_{K^-} + g_{\omega K}\,\omega_0 + g_{\rho K}\,\rho_0 + e\,A_0)^2] K^* \tag{2.18}$$

in the mean-field form (approximation). Here $E_{K^-} = \mathrm{i}\,\partial_0 K^*$ and $<: \, . \, :>$ denotes the expectation value of a normal ordered product of field operators in the ground state $|FK^- >$, which is Fermi sea of filled nucleon states and one antikaon.

The conserved currents serve as proper normalization conditions for the baryon and kaon densities. Namely

$$\int \mathrm{d}^3x\, \rho_N = \int \mathrm{d}^3x \; <: \psi_i^\dagger \psi_i :> = A \tag{2.19}$$

$$\int \mathrm{d}^3x\, \rho_{K^-} = \int \mathrm{d}^3x \; 2(E_{K^-} + g_{\omega K}\,\omega_0 + g_{\rho K}\,\rho_0 + e\,A_0) K^* K = 1\,, \tag{2.20}$$

where A is the nucleon number.

2.2 Numerical solution

Although the baryon field is still an operator, the meson fields are classical. It means that equations (2.13) are linear and we may seek normal-mode solutions of the form

$$\psi_i(x) = e^{-\mathrm{i}\,\varepsilon_i t} \psi_i(\vec{x})\,.$$

This leads to

$$\mathcal{H}\,\psi_i(\vec{x}) = \varepsilon_i\,\psi_i(\vec{x}) \\ \mathcal{H} = [-\mathrm{i}\,\alpha_j \nabla_j + (m_N + g_{\sigma N}\,\sigma)\beta + g_{\omega N}\,\omega_0 + g_{\rho N}\,\tau_3 \rho_0 + e\,\tfrac{1}{2}(1+\tau_3) A_0]\,, \tag{2.21}$$

which defines the single-particle Dirac Hamiltonian $\mathcal{H}$. Expecting both positive and negative energy solutions $u_\alpha(\vec{x})$ and $v_\alpha(\vec{x})$, the baryon field operator can be expanded as

$$\hat{\psi}(\vec{x}) = \sum_\alpha \hat{a}_\alpha u_\alpha(\vec{x}) + \hat{b}_\alpha^\dagger v_\alpha(\vec{x}) \tag{2.22}$$

in the Schrödinger picture. The operators $\hat{a}_\alpha^\dagger$ and $\hat{b}_\alpha^\dagger$ may by interpreted as creation operators for baryons and antibaryons. They satisfy the well-known anticommutation relations for fermions. The label α specifies the full set of quantum numbers describing the single-particle solutions. Since the system is assumed spherically symmetric and parity conserving, α contains the usual angular momentum and parity quantum numbers (for details see e.g. Ref. [37]).

Briefly, if we define the single-particle angular momentum operator as

$$\vec{J} = \vec{L} + \vec{S} = \vec{x} \times \vec{p} + \frac{1}{2}\vec{\Sigma}\,, \tag{2.23}$$

where $\Sigma^i = (\mathrm{i}/2)\varepsilon_{ijk}\gamma^j\gamma^k$ or

$$\vec{\Sigma} = \begin{pmatrix} \vec{\sigma} & 0 \\ 0 & \vec{\sigma} \end{pmatrix} \tag{2.24}$$

it is easy to show that $\mathcal{H}$ is rotationally invariant, i.e. :

$$[\mathcal{H}, J_i] = [\mathcal{H}, \vec{J}^2] = 0 \quad \text{for} \quad i = 1, 2, 3\,. \tag{2.25}$$

Thus the familiar j and m quantum numbers of the angular momentum may be used to label the states. In addition, although, $\vec{L}^2$ does not commute with $\mathcal{H}$, the spin operator $\vec{S}^2 = \vec{\Sigma}^2/4$ obeys $[\mathcal{H}, \vec{S}^2] = 0$. So the spin $s = 1/2$ is a constant of motion. Moreover, by defining the operator

$$\mathcal{K} = \gamma^0[\vec{\Sigma} \cdot \vec{J} - 1/2] = \gamma^0[\vec{\Sigma} \cdot \vec{L} + 1] \tag{2.26}$$

it is straightforward to show that $[\mathcal{H}, \mathcal{K}] = 0$, which provides another constant of motion. This is essentially a consequence of parity conservation.

The eigenvalues $(-\kappa)$ of the operator $\mathcal{K}$ are particularly useful. Since

$$\mathcal{K}^2 = \vec{L}^2 + \vec{\Sigma} \cdot \vec{L} + 1 = \vec{J}^2 + 1/4 \tag{2.27}$$

it follows that

$$\kappa = \pm(j + 1/2) \tag{2.28}$$

and κ is a nonzero integer. If we define upper and lower two-component wave functions by

$$\psi = \begin{pmatrix} \psi_A \\ \psi_B \end{pmatrix}\,, \tag{2.29}$$

and act on this wave function with $\mathcal{K}$

$$\mathcal{K}\psi = -\kappa\psi = \begin{pmatrix} -\kappa\psi_A \\ -\kappa\psi_B \end{pmatrix} = \begin{pmatrix} (\vec{\sigma} \cdot \vec{L} + 1)\psi_A \\ -(\vec{\sigma} \cdot \vec{L} + 1)\psi_B \end{pmatrix}\,, \tag{2.30}$$

we find that ψ_A and ψ_B are eigenstates of $(\vec{\sigma} \cdot \vec{L} + 1)$ with opposite eigenvalues. Since $\vec{L}^2 = \vec{J}^2 - \vec{\Sigma} \cdot \vec{L} - 3/4$, it follows that

$$\begin{aligned} \vec{L}^2\psi_A &= [(j + 1/2)^2 + \kappa]\psi_A \equiv l_A(l_A + 1)\psi_A \\ \vec{L}^2\psi_B &= [(j + 1/2)^2 - \kappa]\psi_B \equiv l_B(l_B + 1)\psi_B\,. \end{aligned} \tag{2.31}$$

Thus, although ψ is not an eigenstate of $\vec{L}^2$, the upper and lower components are separately eigenstates, and for given j and κ, the values of l may be determined from

$$\begin{aligned} j(+1) - l_A(l_A + 1) + 1/4 &= -\kappa \\ j(+1) - l_B(l_B + 1) + 1/4 &= \kappa\,. \end{aligned} \tag{2.32}$$

Since the two-component wave functions have fixed j and $s = 1/2$, l_A and l_B must be $j \pm 1/2$. Their angular momentum and spin parts are therefore simply spherical harmonics

$$\Phi_{\kappa m} = \sum_{m_l m_s} < l\, m_l\, 1/2\, m_s | l\, 1/2\, j\, m > Y_{l\, ml}(\theta, \phi) \chi_{m_s}$$

$$j = |\,\kappa\,| - 1/2, \quad l = \begin{cases} \kappa & \kappa > 0 \\ -(\kappa + 1) & \kappa < 0 \end{cases} , \tag{2.33}$$

where $Y_{l\, m_l}$ is a spherical harmonics and χ_{m_s} is a two-component Pauli spinor. For a given κ, (2.28) and the first relation in (2.32) uniquely determine j and l, as indicated in (2.33). Thus the single-particle wave functions in a central, parity-conserving field may be written as

$$\psi_\alpha(\vec{x}) = \psi_{n\kappa m t}(\vec{x}) = \begin{pmatrix} \mathrm{i}\,[G_{n\kappa t}(r)/r]\Phi_{\kappa m} \\ -[F_{n\kappa t}(r)/r]\Phi_{-\kappa m} \end{pmatrix} \zeta_t\,. \tag{2.34}$$

Since $\mathcal{H}$ also commutes with the isospin operator T_3 and $\vec{T}^2$, the states may be labeled by their charge or isospin projection t ($t = 1/2$ for protons, $t = -1/2$ for neutrons), and ζ_t is a two-component isospinor. The principal quantum number is denoted by n. The phase choice in (2.34) leads to real bound state wave functions F and G for real potentials in (2.21).

Given the general form of the solutions (2.34), we may now evaluate the local source terms in the meson field equations. We assume that the ground state consists of filled shells up to some n and κ. This is consistent with spherical symmetry and is appropriate for doubly magic nuclei. In addition, we assume that all bilinear products of baryon operators are normal ordered.

With these assumptions, the baryon density becomes

$$\begin{aligned} \rho_N(\vec{x}) &= < FK^- | : \hat{\psi}^\dagger(\vec{x}) \hat{\psi}(\vec{x}) : | FK^- > \\ &= \sum_\alpha^{occ} u_\alpha^\dagger(\vec{x})\, u_\alpha(\vec{x}) \\ &= \sum_a^{occ} \left(\frac{2j_a + 1}{4\pi r^2} \right) [\,|G_a(r)|^2 + |F_a(r)|^2\,]\,, \end{aligned} \tag{2.35}$$

where $a \equiv \{n, \kappa, t\}$ denotes remaining quantum numbers. The other densities may be calculated analogously.

With these results, we rewrite the meson field equations as

$$\begin{aligned} (\frac{\mathrm{d}^2}{\mathrm{d}r^2} + \frac{2}{r}\frac{\mathrm{d}}{\mathrm{d}r} - m_\sigma^2)\,\sigma_0(r) &= g_{\sigma N}\,\rho_s(r) + g_2\,\sigma_0^2(r) + g_3\,\sigma_0^3(r) + g_{\sigma K}\,m_K K^*(r) K(r) \\ &= g_{\sigma N} \sum_a^{occ} \left(\frac{2j_a + 1}{4\pi r^2} \right) [\,|G_a(r)|^2 - |F_a(r)|^2\,] \\ &\quad + g_2\,\sigma_0^2(r) + g_3\,\sigma_0^3(r) + g_{\sigma K}\,m_K K^*(r) K(r)\,. \end{aligned} \tag{2.36}$$

$$
\begin{aligned}
(\frac{\mathrm{d}^2}{\mathrm{d}r^2}+\frac{2}{r}\frac{\mathrm{d}}{\mathrm{d}r}-m_\omega^2)\,\omega_0(r) &= -\,g_{\omega N}\,\rho_N(r)+d\,\omega_0^3(r)+g_{\omega K}\,\rho_{K^-}(r)\\
&= -\,g_{\omega N}\sum_a^{occ}\left(\frac{2j_a+1}{4\pi r^2}\right)[\,|G_a(r)|^2+|F_a(r)|^2]\\
&\quad +d\,\omega_0^3(r)+g_{\omega K}\,\rho_{K^-}(r) \qquad (2.37)\\
(\frac{\mathrm{d}^2}{\mathrm{d}r^2}+\frac{2}{r}\frac{\mathrm{d}}{\mathrm{d}r}-m_\rho^2)\,\rho_0(r) &= -\,g_{\rho N}\,\rho_3(r)+g_{\rho K}\,\rho_{K^-}(r)\\
&= -\,g_{\rho N}\sum_a^{occ}\left(\frac{2j_a+1}{4\pi r^2}\right)[\,|G_a(r)|^2+|F_a(r)|^2](-1)^{t_a-1/2}\\
&\quad +g_{\rho K}\,\rho_{K^-}(r) \qquad (2.38)\\
(\frac{\mathrm{d}^2}{\mathrm{d}r^2}+\frac{2}{r}\frac{\mathrm{d}}{\mathrm{d}r})\,A_0(r) &= -\,e\,\rho_p(r)+e\,\rho_{K^-}(r)\\
&= -\,e\sum_a^{occ}\left(\frac{2j_a+1}{4\pi r^2}\right)[\,|G_a(r)|^2+|F_a(r)|^2](t_a+1/2)\\
&\quad +e\,\rho_{K^-}(r)\,, \qquad (2.39)
\end{aligned}
$$

where the densities are given by

$$
\begin{aligned}
\rho_s &= <:\bar{\psi}_i\psi_i:> \qquad (2.40)\\
\rho_N &= <:\psi_i^\dagger\psi_i:> \qquad (2.41)\\
\rho_3 &= <:\psi_i^\dagger\tau_3\psi_i:> \qquad (2.42)\\
\rho_p &= <:\psi_i^\dagger\frac{1-\tau_3}{2}\psi_i:> \qquad (2.43)\\
\rho_{K^-} &= 2\,(E_{K^-}+g_{\omega K}\,\omega_0+g_{\rho K}\,\rho_0+e\,A_0)K^*K\,. \qquad (2.44)
\end{aligned}
$$

The equations for baryon wave functions follow immediately upon substituting (2.34) into (2.21) :

$$
\begin{aligned}
&\frac{\mathrm{d}}{\mathrm{d}r}G_a(r)+\frac{\kappa}{r}\,G_a(r)-[E_a-g_{\omega K}\,\omega_0(r)-2\,t_a g_{\rho N}\,\rho_0(r)\\
&\qquad -(t_a+\frac{1}{2})\,e\,A_0(r)+M+g_{\sigma N}\,\sigma_0(r)]F_a(r)=0 \qquad (2.45)\\
&\frac{\mathrm{d}}{\mathrm{d}r}F_a(r)-\frac{\kappa}{r}\,G_a(r)+[E_a-g_{\omega K}\,\omega_0(r)-2\,t_a g_{\rho N}\,\rho_0(r)\\
&\qquad -(t_a+\frac{1}{2})\,e\,A_0(r)-M-g_{\sigma N}\,\sigma_0(r)]G_a(r)=0\,. \qquad (2.46)
\end{aligned}
$$

The normalization condition for nucleons now reads

$$
\int_0^\infty \mathrm{d}r\,(|G_a(r)|^2+|F_a(r)|^2)=1\,. \qquad (2.47)
$$

The equations (2.18), (2.36)-(2.46) are coupled nonlinear differential equations that have to be solved by an iterative procedure. For a given trial set of meson fields, the Dirac equations (2.45) and (2.46) are solved by Runge-Kutta integration, integrating outward from the origin and inward from large r, matching solutions at some intermediate radius to determine the eigenvalue E_a. Analytic solutions in the regions of large and small r allow proper boundary conditions to be imposed. The Klein-Gordon equation for the antikaon is solved with this trial set of meson fields as well, with the reasonable estimate of the antikaon energy E_{K^-}.

Once the baryon and antikaon wave functions are determined, the source terms in the meson Klein-Gordon equations are calculated and the meson fields recomputed by integrating over the static Green's function

$$D(r, r'; m_i) = -\frac{1}{m_i r r'} \sinh(m_i r_<) \exp(-m_i r_>) \,. \tag{2.48}$$

This Green's function embodies the boundary conditions of exponential decay at large r and vanishing slope for the fields at origin. For example, the solution of equation (2.36) for the scalar field reads

$$\begin{aligned} \sigma_0(r) = & \int_0^\infty \mathrm{d}r' r'^2 [g_{\sigma N}\, \rho_s(r') + g_2\, \sigma_0^2(r') + g_3\, \sigma_0^3(r') + g_{\sigma K}\, m_K K^*(r') K(r')] \times \\ & \times D(r, r'; m_\sigma) \,. \end{aligned} \tag{2.49}$$

The new meson fields are then introduced to the equations of motion for nucleons and the antikaon. The whole procedure is repeated until self-consistency is achieved.

The total energy of the system is determined by :

$$\begin{aligned} E \equiv & < FK^- | : \hat{H} : | FK^- > = \int \mathrm{d}^3x \; < FK^- | : p_i \dot{q}_i - \mathcal{L}^{MFT} : | FK^- > \\ = & \int \mathrm{d}^3x \; < FK^- | : \bar{\psi}_i \mathrm{i}\, \partial_0 \gamma^0 \psi_i + E_{K^-} \rho_{K^-} - \mathcal{L}^{(MFT)} : | FK^- > \\ = & \int \mathrm{d}^3x \, \{ \frac{1}{2}[(\nabla \sigma_0)^2 + m_\sigma \sigma_0^2] - \frac{1}{2}[(\nabla \omega_0)^2 + m_\omega \omega_0^2] - \frac{1}{2}[(\nabla \rho_0)^2 + m_\rho \rho_0^2] - \frac{1}{2}(\nabla A_0)^2 \\ & + \frac{1}{3} g_2 \sigma_0^3 + \frac{1}{4} g_3 \sigma_0^4 + \frac{1}{4} d\, \omega_0^4 \\ & + < FK^- | : \bar{\psi}_i (-\mathrm{i}\, \partial_j \gamma^j + m_N + g_{\sigma N}\, \sigma_0 + g_{\omega N}\, \omega_0 + g_{\rho N}\, \rho_0 \tau_3 \rho_0 + e\, \frac{1 - \tau_3}{2} A_0) \psi_i : | FK^- > \\ & + \nabla_j K^* \nabla_j K + m_K^2 K^* K + g_{\sigma K}\, m_K \sigma_0 K^* K - (E_{K^-} + g_{\omega K}\, \omega_0 + g_{\rho K}\, \rho_0 + e\, A_0)^2 K^* K \\ & + E_{K^-} \rho_{K^-} \} \,. \end{aligned} \tag{2.50}$$

The terms involving the baryon fields are evaluated using the Dirac equation (2.5), with the result

$$\int \mathrm{d}^3x \sum_a^{occ} E_a \left(\frac{2 j_a + 1}{4\pi^2} \right) [\, |G_a(r)|^2 + |F_a(r)|^2] = \sum_a^{occ} E_a (2 j_a + 1) \,, \tag{2.51}$$

which follows from the normalization condition (2.47). For the meson terms, the exponential decay of the fields at large distances permits the following partial integration :

$$\int \mathrm{d}^3x\,\frac{1}{2}[(\nabla\sigma_0)^2+m_\sigma\sigma_0^2] = \frac{1}{2}\int \mathrm{d}^3x\,\sigma_0[-\triangle\sigma_0+m_\sigma\sigma_0^2]$$
$$= \frac{1}{2}\int \mathrm{d}^3x\,[-g_{\sigma N}\,\rho_s - g_2\,\sigma^2 - g_3\,\sigma^3 - g_{\sigma K}\,m_K K^* K]\,, \qquad (2.52)$$

where the final equality follows from the equation (2.14). Similar manipulation with the other fields and using the K^- normalization condition (2.20) allows us to write

$$\begin{aligned} E =& \sum_a^{occ} E_a(2j_a+1) + E_{K^-} \\ & - \frac{1}{2}\int \mathrm{d}^3x\ (g_{\sigma N}\,\sigma\,\rho_s + g_{\omega N}\,\omega_0\,\rho_N + g_{\rho N}\,\rho_0\,\rho_3 + e\,A_0\,\rho_p) \\ & + \frac{1}{2}\int \mathrm{d}^3x\,(-\frac{1}{3}g_2\sigma^3 - \frac{1}{2}g_3\sigma^4 + \frac{1}{2}d\,\omega_0^4) \\ & + \frac{1}{2}\int \mathrm{d}^3x\,[(g_{\omega K}\,\omega_0 + g_{\rho K}\,\rho_0 + e\,A_0)\rho_{K^-} - g_{\sigma K}\,m_K\sigma K^* K]\,. \end{aligned} \qquad (2.53)$$

The traditional RMF approach does not describe the instability of K^- and its absorption in the nuclear medium. In order to include this phenomenon the imaginary part of the optical potential was taken in a phenomenological $t\rho$ form [18], where its depth was fitted to the K^-–atomic data [20] and the nuclear density ρ was calculated within the RMF model. The presence of the K^- leads to the increase of the nuclear density and consequently to increased widths Γ_{K^-}, particularly for the deeply bound states. On the other hand, the phase space available for the decay products is reduced for deeply bound states, which will act to decrease the calculated widths. Thus, suppression factors multiplying the imaginary part of the optical potential were introduced from phase-space considerations, taking into account the binding energy of the antikaon for the initial decaying state, and assuming two-body final-state kinematics for the decay products. Two absorption channels were considered. The dominant one for absorption at rest is due to pionic conversion modes on a single nucleon :

$$K^- N \to \pi\Sigma, \pi\Lambda \qquad (\sim 80\%)\,, \qquad (2.54)$$

with thresholds about 100 MeV and 180 MeV, respectively, below the K^-N total mass. The corresponding density-independent suppression factor is given by

$$f_1 = \frac{M_{01}^3}{M_1^3}\sqrt{\frac{[M_1^2-(m_\pi+m_Y)^2][M_1^2-(m_\pi-m_Y)^2]}{[M_{01}^2-(m_\pi+m_Y)^2][M_{01}^2-(m_\pi-m_Y)^2]}}\,\Theta(M_1-m_\pi-m_Y)\,, \qquad (2.55)$$

where $M_{01}=m_K+m_N$, $M_1=M_{01}-B_{K^-}$ and $B_{K^-}=B({}^A ZK^-)-B({}^A Z)$ is the binding energy of the K^- in the combined K^-–nuclear system ${}^A ZK^-$. The second absorption channel is due to non-pionic absorption modes on two nucleons :

$$K^- NN \to YN \qquad (20\%)\,, \qquad (2.56)$$

with thresholds about $m_\pi = 140$ MeV lower than the single-nucleon threshold. This second channel represents in our model all the multi-nucleon absorption modes which are not resolved by experiment. The corresponding suppression factor is given by

$$f_2 = \frac{M_{02}^3}{M_2^3}\sqrt{\frac{[M_2^2-(m_N+m_Y)^2][M_2^2-(m_N-m_Y)^2]}{[M_{02}^2-(m_N+m_Y)^2][M_{02}^2-(m_N-m_Y)^2]}}\,\Theta(M_2-m_N-m_Y)\,, \tag{2.57}$$

where $M_{02} = m_K + 2m_N$, $M_2 = M_{02} - B_{K^-}$. The branching ratios (quoted above in parentheses) are known from bubble-chamber experiments [38].

Since Σ final states dominate both the pionic and non-pionic channels [38], the hyperon Y was here taken as $Y = \Sigma$. Allowing Λ hyperons would foremost add conversion width to K^- states bound in the region $B_{K^-} \sim 100 - 180$ MeV. For the combined suppression factor we assumed a mixture of 80% mesonic and 20% non-mesonic decay [38], i.e.

$$f = 0.8 f_1 + 0.2 f_2 \tag{2.58}$$

In the calculations below, a residual value $f = 0.02$ was assumed when both f_1 and f_2 vanish.

In order to include the above described scheme we modified the Klein-Gordon equation (2.18) for the K^- as follows :

$$[-\triangle + m_K^2 + V_{opt}]K^* = 0\,, \tag{2.59}$$

where the optical potential is given by

$$V_{opt} = g_{\sigma K}\, m_K \sigma - (\widetilde{E}_{K^-} + g_{\omega K}\,\omega_0 + g_{\rho K}\,\rho_0 + e\,A_0)^2 - 2\,\mathrm{i} f t \rho_N\,, \tag{2.60}$$

and $\widetilde{E}_{K^-}$ denotes complex energy

$$\widetilde{E}_{K^-} = E_{K^-} + \mathrm{i}\,\frac{\Gamma_{K^-}}{2}. \tag{2.61}$$

3 Results and discussion

The main aim of the present work was to develop the RMF model describing interaction of K^- with nucleus including, in addition to previous calculations of Mareš et al. [18], the exchange of the ρ-meson. We studied the effect of the ρ-meson on the predictions of K^-–nuclei properties, which has not been studied up to now. We made calculations of $^{208}\mathrm{Pb}K^-$, where a distinct effect due to large $(N-Z)$ could be expected.

parameter / set	HS	NL-SH	TM1
m_N (MeV)	939.0	939.0	938.0
m_σ (MeV)	520.0	526.09	511.198
m_ω (MeV)	783.0	783.0	783.0
m_ρ (MeV)	770.0	763.0	770.0
$g_{\sigma N}$	10.47	10.444	10.0289
$g_{\omega N}$	13.80	12.945	12.6139
$g_{\rho N}$	8.07	8.766	9.2644
g_2 (fm^{-1})	0.0	-6.9099	-7.2325
g_3	0.0	-15.8337	0.6183
d	0.0	0.0	71.3075

Table 1: Used parameter sets of the Lagrangian density.

The calculations were carried out using one linear (HS [39]) and two nonlinear (NL-SH [40] and TM1 [41]) Lagrangian density parameter sets presented in Table 1. The linear parametrizations are in general characterized by a high value of incompressibility[4] and significantly better stability of numerical solution in comparison with nonlinear parametrizations, which on the other hand offer better description of nuclear properties. For detailed discussion see Ref. [35].

The next step is to specify the kaon coupling constants (to the meson fields). In this work the $g^0_{\omega K} = 1/3\, g_{\omega N}$ and $g^0_{\rho K} = 1/3\, g_{\rho N}$ were taken from simple quark model, which comes out from naive counting of non-strange quarks in K^- with respect to those in nucleon [42]. The coupling constant $g^0_{\sigma K} = 0.233\, g_{\sigma N}$ was fitted to reproduce K^-–atom data [20]. It is to be noted that these values $g^0_{\sigma K}$, $g^0_{\omega K}$, $g^0_{\rho K}$ were used as a "reference" point of our calculations. In order to produce different values of binding energies a particular way of varying the coupling constants was used. Starting from $g_{iK} = \alpha_i\, g^0_{iK} = 0$ $(i = \sigma, \omega)$ we first scaled up the α_ω up to $\alpha_\omega = 1$ and afterwards scaled up the α_σ until the binding energy $B_{K^-} \sim 150$ MeV was reached.

In this paragraph we discuss some results of calculated K^-–nuclear bound states properties, such as their binding energies and widths. In particular we studied ρ-meson influence on these observables. Moreover, we calculated the average nuclear density[5], the nuclear

[4] $K_\infty = 9\rho_0^2 \frac{\mathrm{d}^2}{\mathrm{d}\rho^2} \frac{E}{A}|_{\rho=\rho_0}$, where ρ_0 is nuclear matter saturation point

[5] $\bar{\rho}_N = \frac{1}{A} \int \mathrm{d}^3x\, \rho^2$

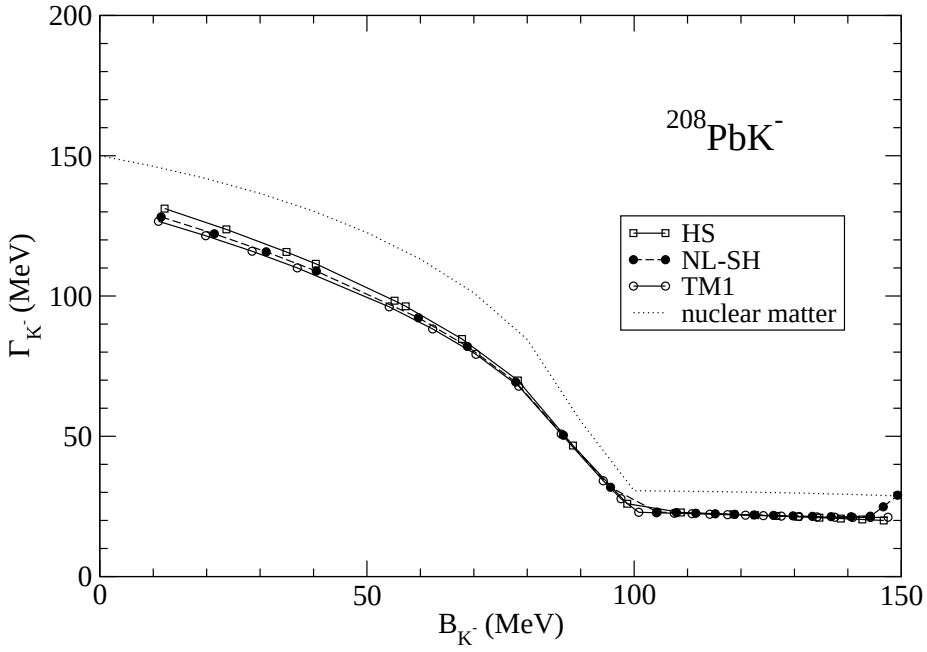

Figure 1: Calculated decay widths Γ_{K^-} of the $1s\,K^-$–nuclear state in ^{208}PbK^- as function of K^- binding energy B_{K^-} for several parameter sets. The dotted line stands for static nuclear matter calculations with $\rho_0 = 0.16$ fm^{-3}.

density and K^- density distributions in order to study the nuclear core polarization due to the presence of the K^-.

Figure 1 shows calculated widths Γ_{K^-} as function of the binding energy B_{K^-} for $1s$ states in ^{208}Pb for the linear (HS) and non-linear (NL-SH, TM1) versions of the RMF model. The dotted line stands for a static nuclear matter limit with $\rho_0 = 0.16$ fm^{-3}. It is clearly seen that the dependence of the width on the binding energy follows the shape for the static nuclear matter limit. This dependence is a primarily consequence of the binding energy dependence on the suppression factor f [18], which falls rapidly until $B_{K^-} \sim 100$ MeV, where the dominant $K^-N \to \pi\Sigma$ vanishes, and stays rather flat within the range $B_{K^-} \sim 100 - 150$ MeV, where the width is governed by the two-nucleon absorption mode $K^-NN \to \Sigma N$. The fact that the widths Γ_{K^-} for ^{208}Pb up to $B_{K^-} \sim 150$ MeV lie under the value for static nuclear matter is a consequence of the lower average nuclear density in lead than the density of nuclear matter (via ρ dependence of the decay width Γ_{K^-}) and of the overlap of the ^{208}Pb– and K^-–wave functions (it is a finite system in comparison with nuclear matter). For lighter nuclei the situation is inverse - results for finite nuclei lie above the result for static nuclear matter. This is a consequence of strong polarization effects of K^- on nucleus (higher nuclear density $\rho > \rho_0$) as shown e.g. by Mareš et al. [18], which are negligible for heavy nuclei such as ^{208}Pb (see further comments on Fig. 3). At the binding energy $B_{K^-} \gtrsim 150$ MeV another phenomenon appears for the non-linear parameter set. The ^{208}Pb single particle energies undergo significant crossings, the maximal nuclear density increases, the K^-–wave function

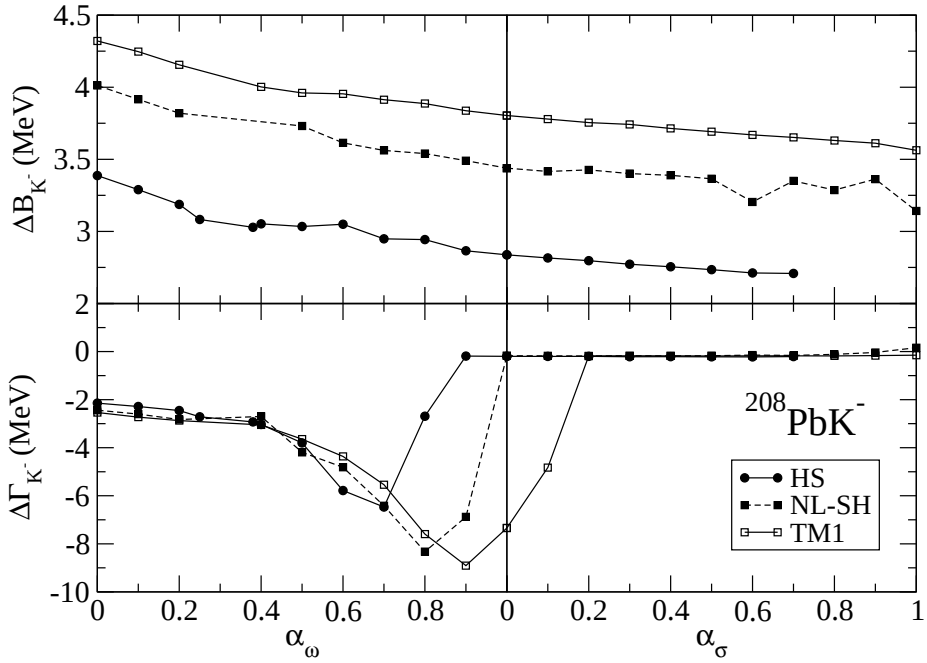

Figure 2: Calculated difference ΔB_{K^-} and $\Delta\Gamma_{K^-}$ between $1s\,K^-$–nuclear state binding energies and decay widths for ^{208}Pb with and without the ρ-meson exchange using several parameter sets.

is more localized in the center of the nucleus, and as a result the nuclear rearrangement energy significantly rises. Finally, it is evident that the obtained widths Γ_{K^-} as function of B_{K^-} are equivalent for all used parametrizations (up to $B_{K^-} \lesssim 150$ MeV).

Fig. 2 shows the calculated difference $\Delta B_{K^-} = B_{K^-}^{(\mathrm{no}\ \rho)} - B_{K^-}^{(\rho)}$ and $\Delta\Gamma_{K^-} = \Gamma_{K^-}^{(\mathrm{no}\ \rho)} - \Gamma_{K^-}^{(\rho)}$ between $1s\,K^-$–nuclear state binding energies and decay widths for ^{208}Pb with and without the ρ-meson exchange. It is seen that the effect of the ρ-meson exchange for higher binding energies B_{K^-} is small even in ^{208}Pb. The difference of the K^- binding energy reaches $\Delta B_{K^-} \sim 3-4$ MeV and fluently falls with increasing coupling constant ratios α_σ and α_ω. The oscillation for $\alpha_\sigma \gtrsim 0.5$ for the NL-SH parameter set are caused by worse convergence of the numerical solution. The effect on the K^- decay width is even smaller. Aside from the region of the substantial decrease of Γ_{K^-} ($\alpha_\omega \sim 0.5 - \alpha_\sigma \sim 0.2$ which corresponds to 60 MeV $< B_{K^-} <$ 100 MeV) the effect is $\Delta\Gamma_{K^-} \sim 0$ MeV. In this region the difference reaches $\Delta\Gamma_{K^-} \sim -10$ MeV. The calculated $\Delta\Gamma_{K^-}$ except the above mentioned region are equivalent for all used parametrizations unlike ΔB_{K^-} which, even if showing the same trend, differ for each parameter set.

The average nuclear density $\bar{\rho}_N$ as function of the K^- binding energy and several parametrizations is shown in Fig. 3. It is evident that the average nuclear density $\bar{\rho}_N$ in ^{208}Pb remains roughly unchanged in the presence of K^-. This feature indicates that the polarization effect of the K^- on heavy nuclei such as ^{208}Pb is very small. For comparison we present results for ^{16}O, where the influence of K^- is more evident. This confirms a strong polarization of the nuclear core for light nuclei. Different results were obtained

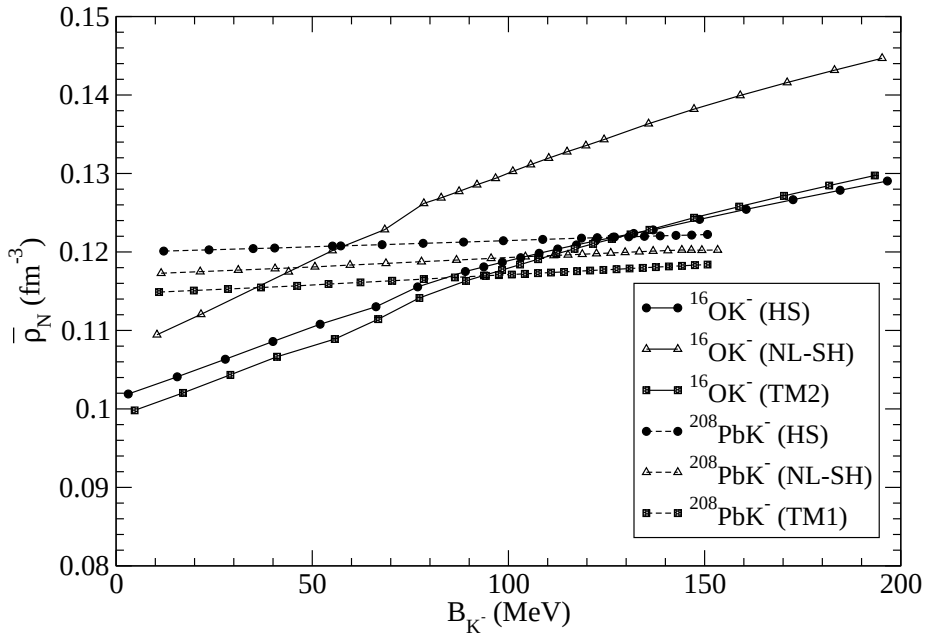

Figure 3: Calculated average nuclear density $\bar{\rho}_N$ for $^{16}\mathrm{O}K^-$ and $^{208}\mathrm{Pb}K^-$ as function of the $1s\,K^-$–nuclear state binding energy B_{K^-} using several parameter sets.

for different parametrizations. This is due to the fact that each parametrization gives slightly different values of "pure" ^{208}Pb characteristics. Moreover, each parametrization has another value of incompressibility therefore non-linear models (lower incompressibility) predict larger changes of $\bar{\rho}_N$ due to the presence of K^-.

Next figures show the calculated nuclear densities ρ_N (Fig. 4(a), 5(a)) and antikaon densities ρ_{K^-} (Fig. 4(b), 5(b)) for the linear HS and non-linear TM1 parametrizations and for several values of the $1s\,K^-$ binding energies. The nuclear density of ^{208}Pb, in the absence of K^-, is given by the dotted curve. While the average nuclear density $\bar{\rho}_N$ in ^{208}Pb remains roughly constant, the nuclear density ρ_N perceptibly increases in the central region of order 2 fm from the origin. For the linear HS parametrization the increase of ρ_N reaches 15% (at the maximal nuclear density) for $B_{K^-} = 150$ MeV, while the K^- density $\rho_{K^-}(0) \sim 0.15$ fm^{-3}. The localization of the nuclear density enhancement is due to the localized $1s\,K^-$ density. The results for the non-linear TM1 parametrization are at least controversial. The value of 50% for the central nuclear density increase seems to be too large. The increase for the non-linear NL-SH parameter set is even larger, which is not presented here. It is most likely due to the level crossing, which takes place in the ^{208}Pb core in the presence of the strongly interacting K^-. This issue clearly calls for further explorations. Nevertheless, it is evident that the results obtained for the TM1 parameter set are equivalent to those for the HS parametrization up to the K^- binding energies $B_{K^-} \lesssim 120$ MeV.

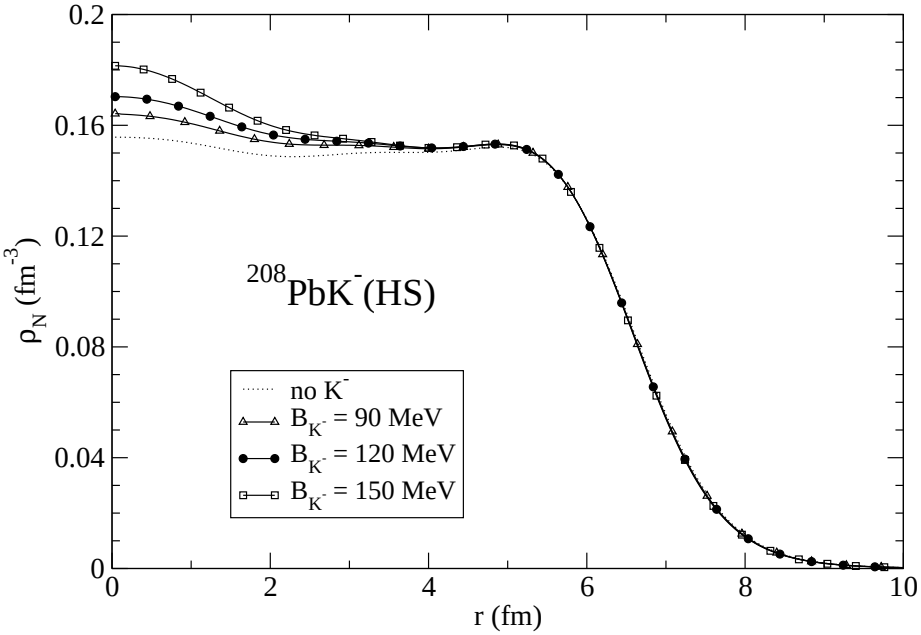

(a) Calculated nuclear density ρ_N for several $1s\,K^-$–nuclear states with specified B_{K^-}. The dotted curve stands for the nuclear density in the absence of K^-.

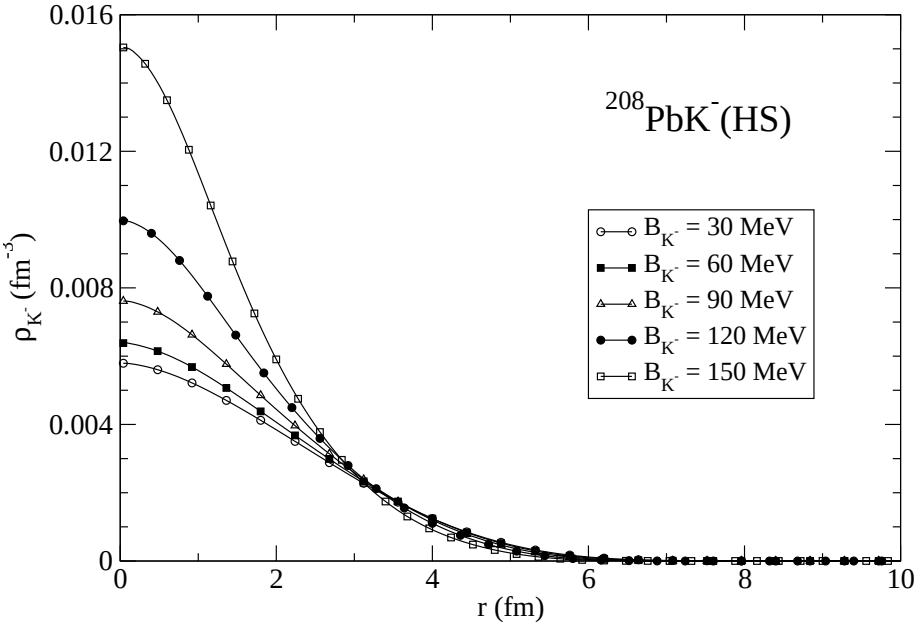

(b) Calculated K^- density ρ_{K^-} for several $1s\,K^-$–nuclear states with specified B_{K^-}.

Figure 4: Calculated nuclear and K^- densities using the linear HS parameter set.

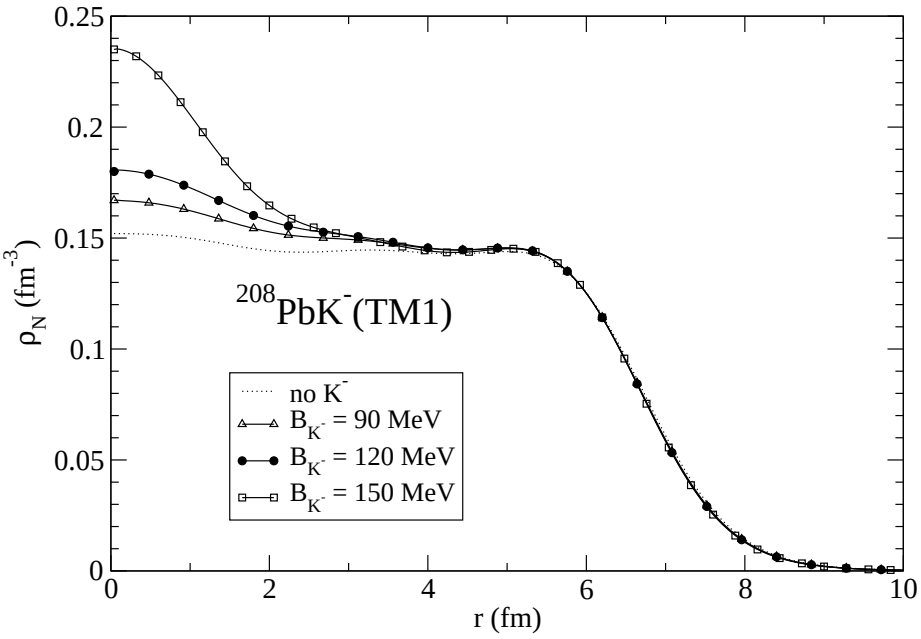

(a) Calculated nuclear density ρ_N for several $1s\,K^-$–nuclear states with specified B_{K^-}. The dotted curve stands for the nuclear density in the absence of K^-.

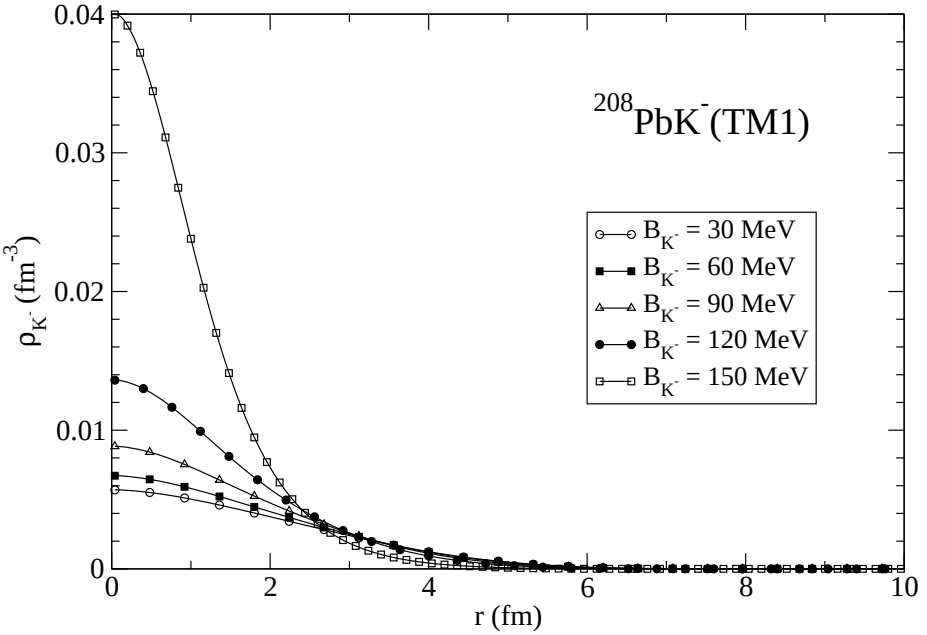

(b) Calculated K^- density ρ_{K^-} for several $1s\,K^-$–nuclear states with specified B_{K^-}.

Figure 5: Calculated nuclear and K^- densities for ^{208}Pb using the non-linear TM1 parameter set.

4 Summary

In the present work we studied the influence of the isovector interaction, mediated by the ρ-meson, on selected characteristics of the $1s\,K^-$–nuclear bound states. The RMF model for the interaction of K^- with a nucleus including the exchange of the ρ-meson was developed and relevant equations of motion were derived. We calculated $^{208}\mathrm{Pb}K^-$ where the most prominent effect of the ρ-meson could be anticipated due to $N \gg Z$. Performed self-consistent calculations covered a wide range of the K^- binding energies ($B_{K^-} \sim 10 - 150$ MeV) in order to establish correlations among calculated properties such as the K^- decay widths, the average nuclear density, the nuclear density and K^- density distributions.

For all used parametrizations an equivalent results were obtained for the dependence of the K^- decay width on its binding energy. The K^- widths are primarily suppressed by the reduced phase space for K^-. In $^{208}\mathrm{Pb}K^-$ they are lower compared to the nuclear matter results as a consequence of the lower average nuclear density in lead.

It has been shown that the influence of the ρ-meson exchange on the K^- binding energy amounts to $\Delta B_{K^-} \sim 4$ MeV and is thus insignificant for higher values of B_{K^-} (e.g. $\Delta B_{K^-} \sim 4\%$ for $B_{K^-} \sim 100$ MeV). All the applied RMF parametrizations predict similar decrease of ΔB_{K^-} with increasing binding energy B_{K^-}, though the absolute values differ. The ρ-meson exchange contribution in the K^- decay width is uniform $\Delta\Gamma_{K^-} \sim 0$ MeV for each parametrization except the region, where Γ_{K^-} undergoes significant changes due to vanishing of dominant decay channel. In this region the difference reaches $\Delta\Gamma_{K^-} \sim -10$ MeV and differs for each parametrization.

The calculations revealed that the average nuclear density in such a heavy nucleus like ^{208}Pb is only little influenced by the presence of K^-. This implies small polarization effects of K^- on the nuclear core unlike the case of light nuclei, such as ^{16}O, where the polarization is more significant. Even though the average nuclear density in ^{208}Pb remains roughly constant, the nuclear density in central region conspicuously rises due to the increase of the $1s\,K^-$ density localization. This enhancement of the maximal nuclear density occurs in a small region of order 2 fm from the origin, which is still well within the nuclear volume, and therefore the average nuclear density is only weakly enhanced as function of the K^- binding energy. The calculated value for the increase of the central nuclear density is 15% for the linear HS and 50% for nonlinear TM1 parameter set. This high value for the TM1 parameter set is likely a consequence of the single particle level crossing, which takes place in the ^{208}Pb core in the presence of the strongly interacting K^-. However, it might also indicate failure of the non-linear models, originally designed for the description of standard nuclei, in this region. This issue clearly calls for further explorations.

Acknowledgments

This work was supported by the GA AVCR grant A100480617.

References

[1] H.V. Klapdor-Kleingrothaus, A. Staudt, Non-Accelerator Particle Physics, Inst. of Physics Publishing, Bristol & Philadelphia, 1995.

[2] B.D. Kaplan and A.E. Nelson, Phys. Lett. B **175** (1986) 57.

[3] A.E. Nelson, B.D. Kaplan, Phys. Lett. B **192** (1987) 193.

[4] F. Laue et al., Phys. Rev. Lett. **82** (1999) 1640.

[5] F. Laue et al., Eur. Phys. J. A **9** (2000) 397.

[6] M. Menzel et al., Phys. Lett. B **495** (2000) 26.

[7] G.E. Brown, C.-H. Lee et al., Nucl Phys. A **567** (1994) 937.

[8] G.Q. Li, C.-H. Lee, G.E. Brown, Nucl. Phys A **625** (1997) 372.

[9] J. Schaffner, I.N. Mishustin, J. Bondorf, Nucl. Phys. A **625** (1997) 325.

[10] J. Schaffner, A. Gal, I.N. Mishustin, H. Stöcker, W. Greiner, Phys. Lett. B **334** (1994) 268.

[11] J. Schaffner, I.N. Mishustin, Phys. Rev. C **53** (1996) 1416.

[12] T. Waas, N. Kaiser, W. Weise, Phys. Lett. B **365** (1996) 12; Phys. Lett. B **379** (1996) 34; N. Kaiser, P.B. Siegel, W. Weise, Nucl. Phys. A **594** (1995) 325; W. Weise, ibid. **610** (1996) 35.

[13] T. Waas, W. Weise, Nucl. Phys. A **625** (1997) 287.

[14] E. Oset, D. Camabera, V.K. Magas, L. Roca, S. Sarkar, M.J. Vicente Vacas, A. Ramos, PRAMANA **53** (1999) 1.

[15] S. Hirenzaki, Y. Okumura, H. Toki, E. Oset, A. Ramos, Phys. Rev. C **61** (2000) 055205.

[16] A. Baca, C. García-Recio, J. Nieves, Nucl. Phys. A **673** (2000) 335.

[17] A. Cieplý, E. Friedman, A. Gal, J. Mareš, Nucl. Phys. A **696** (2001) 173.

[18] J. Mareš, E. Friedman, A. Gal, Nucl. Phys. A **770** (2006) 84.

[19] E. Friedman, A. Gal, C.J. Batty, Phys. Lett B **308** (1993) 6; E. Friedman, A. Gal, C.J. Batty, Phys. Lett. B **579** (1994) 518.

[20] E. Friedman, A. Gal, J. Mareš, A. Cieplý, Phys. Rev. C **60** (1999) 024314.

[21] Y. Akaishi, A. Doté, T. Yamazaki, Phys. Lett. B **613** (2005) 140 and references therein.

[22] T. Suzuki, H. Bhang, G. Franklin, K. Gomikawa, R.S. Hayano, T. Hayashi, K. Ishikawa, S. Ishimoto, K. Itahashi, M. Iwasaki, T. Katayama, Y. Kondo, Y. Matsuda, T. Nakamura, S. Okada, H. Outa, B. Quinn, M. Sato, M. Shindo, H. So, P. Strasser, T. Sugimoto, K. Suzuki, S. Suzuki, D. Tomono, A.M. Vinodkumar, E. Widmann, T. Yamazaki, T. Yoneyama, Phys. Lett. B **597** (2004) 263.

[23] T. Suzuki, H. Bhang, G. Franklin, K. Gomikawa, R.S. Hayano, T. Hayashi, K. Ishikawa, S. Ishimoto, K. Itahashi, M. Iwasaki, T. Katayama, Y. Kondo, Y. Matsuda, T. Nakamura, S. Okada, H. Outa, B. Quinn, M. Sato, M. Shindo, H. So, P. Strasser, T. Sugimoto, K. Suzuki, S. Suzuki, D. Tomono, A.M. Vinodkumar, E. Widmann, T. Yamazaki, T. Yoneyama, Nucl. Phys. A **754** (2005) 375c.

[24] T. Kishimoto, T. Hayakawa, S. Ajimura, S. Minami, A. Sakaguchi, Y. Shimizu, R.E. Chrien, M. May, P. Pile, A. Rusek, R. Sutter, H. Noumi, H. Tamura, M. Ukai, Y. Miura, K. Tanida, Nucl. Phys. A **754** (2005) 383c.

[25] M. Agnello, G. Beer, L. Benussi, M. Bertani, S. Bianco, E. Botta, T. Bressani, L. Busso, D. Calvo, P. Camerini, P. Cerello, B. Dalena, F. De Mori, G. D Erasmo, D. Di Santo, F.L. Fabbri, D. Faso, A. Feliciello, A. Filippi, V. Filippini, E.M. Fiore, H. Fujioka, P. Gianotti, N. Grion, V. Lucherini, S. Marcello, T. Maruta, N. Mirfakhrai, O. Morra, T. Nagae, A. Olin, H. Outa, E. Pace, M. Palomba, A. Pantaleo, A. Panzarasa, V. Paticchio, S. Piano, F. Pompili, R. Rui, G. Simonetti, H. So, S. Tomassini, A. Toyoda, R. Wheadon, A. Zenoni, Phys. Rev. Lett. **94** (2005) 212303.

[26] V.K. Magas, E. Oset, A. Ramos, H. Toki, Phys. Rev. C **74** (2006) 025206.

[27] M.H. Johnson, E. Teller, Phys. Rev. **98** (1955) 783.

[28] H.P. Duerr, E. Teller, Phys. Rev. **101** (1956) 494.

[29] H.P. Duerr, Phys. Rev. **103** (1956) 469.

[30] J.D. Walecka, Ann. Phys. **83** (1974) 491.

[31] B.D. Serot, J.D. Walecka, Adv. Nucl. Phys. **16** (1986) 1.

[32] P. Quentin, H. Flocard, Ann. Rev. Nucl. Part. Sci. **28** (1978) 523.

[33] J. Decharge, D. Gogny, Phys. Rev C **21** (1980) 1568.

[34] Time-Dependent Hartee-Fock and Beyond, Lecture Notes in Physics, Vol. **171**, eds. K. Goeke, P.-G. Reinhard, Springer, Berlin, 1982.

[35] P.-G. Reinhard, Rep. Progr. Phys. **52** (1989) 439.

[36] S. Weinberg, The Quantum Theory of Fields, Vol. 1, Cambridge University Press, 1995.

[37] J.D. Björken, S.D. Drell, Relativistic Quantum Mechanics, McGraw-Hill, New York, 1964.

[38] C. Vander Velde-Wilquet, J. Sacton, J.H. Wickens, D.N. Tovee, D.H. Davis, Nuovo Cimento A **39** (1977) 538.

[39] C.J. Horowitz, B.D. Serot, Nucl. Phys. A **368** (1981) 503.

[40] M.M. Sharma, M.A. Nagarajan, P. Ring, Phys. Lett. B **312** (1993) 377.

[41] Y. Sugahara, H. Toki, Nucl. Phys. A **579** (1994) 557.

[42] B.K. Jennings, Phys. Lett. B **246** (1990) 325.

Appendix A : Notation and conventions

We adhere primarily to the conventions of Serot and Walecka [31]. Physical units are chosen with $\hbar = c = 1$. Contravariant x^μ and covariant x_μ four-vectors are written as

$$x \equiv x^\mu = (t, \vec{x}), \qquad x_\mu = (t, -\vec{x}) \tag{A.1}$$

$$\partial^\mu \equiv \frac{\partial}{\partial x_\mu} = \left(\frac{\partial}{\partial t}, -\nabla\right), \qquad \partial_\mu \equiv \frac{\partial}{\partial x^\mu} = \left(\frac{\partial}{\partial t}, \nabla\right). \tag{A.2}$$

The Dirac equation for a free particle of mass M reads

$$(\mathrm{i}\,\gamma_\mu \partial^\mu - M)\psi = (\mathrm{i}\,\not{\partial} - M)\psi = 0, \tag{A.3}$$

where we use Feynman "slash" notation $\not{a} \equiv a_\mu \gamma^\mu$. The gamma matrices obey

$$\gamma^\mu \gamma^\nu + \gamma^\nu \gamma^\mu = \{\gamma^\mu, \gamma^\nu\} = 2\, g^{\mu\nu}, \tag{A.4}$$

where $g^{\mu\nu}$ is a metric tensor given by

$$g^{\mu\nu} = \begin{pmatrix} 1 & 0 & 0 & 0 \\ 0 & -1 & 0 & 0 \\ 0 & 0 & -1 & 0 \\ 0 & 0 & 0 & -1 \end{pmatrix}, \tag{A.5}$$

and in the standard (Dirac-Pauli) realization are written as

$$\gamma^0 = \begin{pmatrix} \mathbb{1} & 0 \\ 0 & -\mathbb{1} \end{pmatrix}, \qquad \vec{\gamma} = \begin{pmatrix} \vec{\sigma} & 0 \\ 0 & -\vec{\sigma} \end{pmatrix}, \tag{A.6}$$

with the Pauli matrices defined by

$$\sigma_1 = \begin{pmatrix} 0 & 1 \\ 1 & 0 \end{pmatrix}, \qquad \sigma_2 = \begin{pmatrix} 0 & -\mathrm{i} \\ \mathrm{i} & 0 \end{pmatrix}, \qquad \sigma_3 = \begin{pmatrix} 1 & 0 \\ 0 & -1 \end{pmatrix}. \tag{A.7}$$

Further, the nucleon and kaon wave functions are considered as isospin doublets, i.e.

$$\psi_i \equiv \begin{pmatrix} \psi_p \\ \psi_n \end{pmatrix}, \tag{A.8}$$

where ψ_p and ψ_n denotes proton and neutron states respectively, and

$$K \equiv \begin{pmatrix} K^+ \\ K^0 \end{pmatrix}, \tag{A.9}$$

where K^+ and K^0 denotes positively charged and neutral kaon respectively.